UC Irvine

UC Irvine Previously Published Works

Title

The seasonality and geographic dependence of ENSO impacts on U.S. surface ozone variability

Permalink

https://escholarship.org/uc/item/6sb011nd

Journal

Geophysical Research Letters, 44(7)

ISSN

0094-8276

Authors

Xu, L
Yu, JY
Schnell, JL
et al.

Publication Date

2017-04-16

DOI

10.1002/2017GL073044

Peer reviewed

eScholarship.org Powered by the California Digital Library
University of California

AGU PUBLICATIONS

Geophysical Research Letters

RESEARCH LETTER
10.1002/2017GL073044

Key Points:
- U.S. surface ozone decreases (increases) during El Niño (La Niña) years with amplitude up to 1.8 ppb per standard deviation of Niño 3.4 index
- The largest ENSO influences on U.S. ozone occur in southern (western) regions during fall (winter to spring) when ENSO develops (decays)
- ENSO affects U.S. surface ozone via chemical processes (dynamic transport) during warm (cold) seasons in two southern (western) regions

Supporting Information:
- Supporting Information S1

Correspondence to:
L. Xu,
lxu16@uci.edu

Citation:
Xu, L., J.-Y. Yu, J. L. Schnell, and M. J. Prather (2017), The seasonality and geographic dependence of ENSO impacts on U.S. surface ozone variability, *Geophys. Res. Lett.*, *44*, 3420–3428, doi:10.1002/2017GL073044.

Received 16 FEB 2017
Accepted 13 MAR 2017
Accepted article online 16 MAR 2017
Published online 15 APR 2017

©2017. American Geophysical Union. All Rights Reserved.

The seasonality and geographic dependence of ENSO impacts on U.S. surface ozone variability

Li Xu[1], Jin-Yi Yu[1], Jordan L. Schnell[1,2], and Michael J. Prather[1]

[1]Department of Earth System Science, University of California, Irvine, California, USA, [2]Now at Program in Atmospheric and Oceanic Sciences, Princeton University, Princeton, New Jersey, USA

Abstract We examine the impact of El Niño–Southern Oscillation (ENSO) on surface ozone abundance observed over the continental United States (U.S.) during 1993–2013. The monthly ozone decreases (increases) during El Niño (La Niña) years with amplitude up to 1.8 ppb per standard deviation of Niño 3.4 index. The largest ENSO influences occur over two southern U.S. regions during fall when the ENSO develops and over two western U.S. regions during the winter to spring after the ENSO decays. ENSO affects surface ozone via chemical processes during warm seasons in southern regions, where favorable meteorological conditions occur, but via dynamic transport during cold seasons in western regions, where the ENSO-induced circulation variations are large. The geographic dependence and seasonality of the ENSO impacts imply that regulations regarding air quality and its exceedance need to be adjusted for different seasons and U.S. regions to account for the ENSO-driven patterns in surface ozone.

1. Introduction

The El Niño–Southern Oscillation (ENSO) is a dominant mode of interannual variability in Earth's climate system. The warm phase of ENSO (i.e., El Niño) is characterized by anomalously warm sea surface temperatures (SST) in the central to eastern Pacific, while its cold phase (i.e., La Niña) displays a similar pattern but with cold SST anomalies. These SST anomalies can alter atmospheric circulations and excite teleconnection patterns [*Bjerknes*, 1969; *Enfield*, 1989] to impact global climate, including the temperature and precipitation patterns over the Unites States [*Ropelewski and Halpert*, 1987; *Mo*, 2010; *Yu et al*., 2012; *Yu and Zou*, 2013; *Liang et al*., 2015]. Such changes in ambient meteorology fields can alter the distribution of atmospheric constituents in the troposphere [*Chandra et al*., 1998, 2002, 2009; *Sudo and Takahashi*, 2001; *Ziemke and Chandra*, 2003; *Zeng and Pyle*, 2005; *Doherty et al*., 2006; *Randel and Thompson*, 2011; *Olsen et al*., 2016] and in the stratosphere [*Randel and Cobb*, 1994]. In terms of ozone, numerous studies have investigated tropospheric column ozone in the tropical Pacific [*Olsen et al*., 2016, and references therein], intercontinental transport of Asian pollution [*Lin et al*., 2014], and stratosphere-troposphere exchange [*Zeng and Pyle*, 2005; *Lin et al*., 2015]. None yet have demonstrated ENSO-related changes in surface ozone in the United States. Surface ozone is a critical pollutant with adverse impacts on human health and vegetation close to the ground, and thus it is of great importance to understand how the ENSO might impact U.S. surface ozone. Such understanding can be used to assess the consequences of possible future changes in ENSO on regional surface ozone as well as to consider a potential alteration of the air quality standard during ENSO years. Here we present the correlations of ENSO with ozone air quality, based on the U.S. Environmental Protection Agency and Canadian measurements of the daily ozone over North America during 1993–2013. Comparing monthly averaged ozone concentrations with ENSO indices allows us to identify the geographic dependence and seasonality of the ENSO influence on U.S. air quality.

2. Data and Analysis Methods

The surface ozone data used in this study is an extended version of the regularly gridded, maximum daily 8 h average (MDA8) surface ozone mixing ratios (ppb) derived by *Schnell et al*. [2015] from hourly surface ozone measurements from air quality networks in North America during 1993–2013. The derived daily MDA8 surface ozone data are gridded at 1°×1° and covers the continental region of North America (24°N–49°N; 67°W–126°W). We first binned the daily MDA8 surface ozone into monthly averages and then removed a linear fit to the monthly ozone data during this 21 year period. The purpose of this detrending is to remove any long-term systematic changes in anthropogenic emissions of ozone precursors (e.g., NO_x) on surface

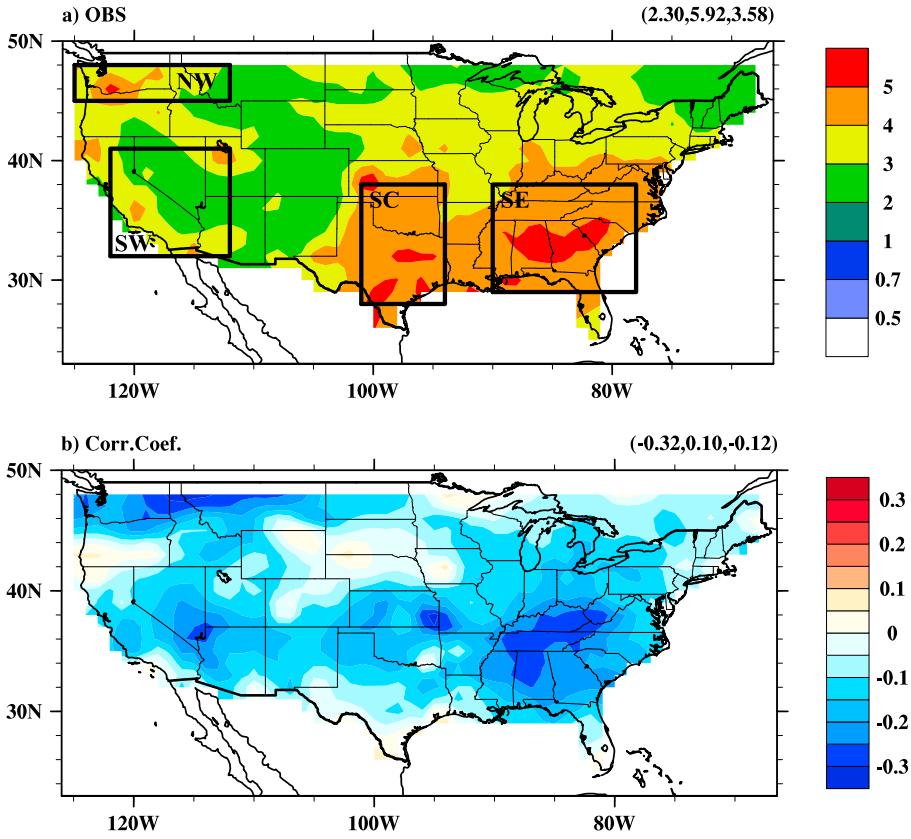

Figure 1. (a) The standard deviation of monthly mean deseasonalized MDA8 surface ozone anomalies from observations and (b) the correlation coefficient between observed ozone anomalies and the Niño 3.4 index. Four regions are marked as black rectangular boxes (i.e., southeastern U.S. (29°N–38°N; 78°W–90°W), south central U.S. (28°N–38°N; 94°W–101°W), southwestern U.S. (32°N–41°N; 112°W–122°W), and northwestern U.S. (45°N–48°N; 112°W–125°W)) are labeled as SE, SC, SW, and NW.

ozone concentrations [e.g., *Jaffe et al.*, 2003; *Leibensperger et al.*, 2008; *Bloomer et al.*, 2009; *Cooper et al.*, 2012; *Strode et al.*, 2015]. Anomalies are calculated as the deviations from 21 year average seasonal cycles.

Meteorological variables used in this study, including monthly surface air temperature, specific humidity, total cloud fraction, 850 hPa geopotential height, 925 hPa meridional wind, and 200 hPa zonal wind, are from National Centers for Environmental Prediction-National Center for Atmospheric Research (NCEP-NCAR) Reanalysis [*Kalnay et al.*, 1996]. An air stagnation index [*Wang and Angell*, 1999] and the Niño 3.4 index are downloaded from the National Oceanic and Atmospheric Administration-National Centers.

3. Results

In terms of the detrended and deseasonalized monthly MDA8 surface ozone anomalies, the U.S. surface ozone variance is largest over four particular regions designated North West (NW), South West (SW), South Central (SC), and South East (SE). The standard deviation of surface ozone along with the four designated regions are plotted in Figure 1a, with a North American average of 3.6 ppb and averages of 3.5, 3.1, 4.7, and 4.7 in regions NW, SW, SC, and SE, respectively. We calculate correlation coefficients (r) between the Niño 3.4 index and surface ozone anomalies for each grid cell (Figure 1b). With a largest absolute value of $r \sim -0.3$ in the SE and SC boxes, it means that about $r^2 \sim 10\%$ of the ozone variance is tied to ENSO. Because largest negative correlations occur where the ozone variance is large, the r^2 describes the fraction of area-weighted ozone variance that is linked to the Niño 3.4 index. This fraction over the North American region gives 1%, while it is slightly higher, 4%, 2%, 1%, and 4%, within the NW, SW, SC, and SE regions, respectively (Figure 1b). Even in regions with larger r, the ENSO correlation represents a small fraction (<5%) of the observed ozone variability. Nevertheless, if ENSO is a causative factor and then it is not random, we can

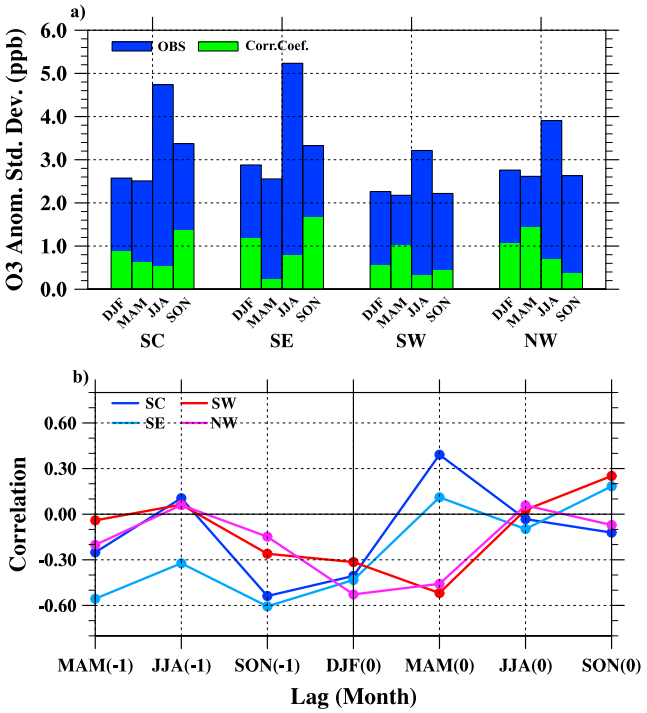

Figure 2. (a) The standard deviation of observed (OBS) and correlation coefficient of derived (Corr.Coef.) monthly anomalous MDA8 surface ozone mixing ratio (ppb) averaged in four regions (i.e., SC, SE, SW, and NW) for four seasons (DJF, MAM, JJA, and SON) drawn from left to right at each region; (b) the lag correlation between observed monthly anomalous MDA8 surface ozone mixing ratio and the wintertime Niño 3.4 index (i.e., DJF) in four regions. The label "(-1)" is used to mark the seasons during the ENSO developing phase, whereas the label "(0)" marks the seasons during the ENSO decaying phase.

estimate the amplitude of surface ozone changes through the ENSO cycle by the product of *r* and ozone standard deviation, which varies from 0.4 ppb (continent-wide average) to 1.8 ppb (SE region) per standard deviation of the Niño 3.4 index on a monthly basis. This is a notable shift on what could be considered baseline ozone and could thus affect threshold exceedances in some regions. The negative correlation coefficients observed over most of the U.S. indicate that the surface ozone abundance decreases during El Niño years but increases during La Niña years. It is worth noting that some regions constantly subjected to deteriorated air quality with high ozone concentrations (e.g., the Northeast Corridor down to mid-Atlantic) exhibit low interannual variability (shown in Figure 1a) as well as little association with ENSO (shown in Figure 1b). This suggests that the ozone variability over the northeastern U.S. may be explained by some other synoptic-scale factors (e.g., variability in the polar jet and associated cold fronts) [*Shen et al*., 2015].

To explore the seasonality of the ENSO influence on U.S. surface ozone, we restrict ourselves to the four selected regions and use the same monthly gridded anomalies but group by season for boreal winter (December-January-February aka DJF; i.e., 21 × 3 winter months), spring (March-April-May aka MAM), summer (June-July-August aka JJA), and fall (September-October-November aka SON). Following the method above, we derive the amplitude of ozone anomalies associated with ENSO based on the correlation coefficient. This amplitude is compared with the standard deviation of the observed monthly ozone in each season in Figure 2a. The largest ozone standard deviation, 3.3 to 5.3 ppb, occurs in summer for all four regions, because summer is the pollution season in most of North America. The greatest amplitude of the ENSO influence on surface ozone, however, is not during summer but during fall for the two southern regions (1.4–1.7 ppb) and during spring for the two western regions (1.0–1.4 ppb).

A tropical ENSO event typically begins in spring, develops during summer and fall, reaches its peak intensity in winter, and decays in the following spring and summer seasons. The evolution and location of the SST anomalies can be different between the developing and decaying phases of the ENSO event [e.g., *Rasmussen and Carpenter*, 1982; *An and Wang*, 2000; *Kao and Yu*, 2009], and as a result, the impact during the seasons of its developing phase can be different from those during the decaying phases [e.g., *Liang et al*., 2016]. To identify whether the largest ENSO influence on the four U.S. regions occurs during the developing or decaying seasons, we perform a lead-lagged correlation analysis between seasonal surface ozone anomalies and the winter (DJF) Niño 3.4 index as shown in Figure 2b. We use the winter Niño 3.4 index to represent the peak time of the ENSO. The magnitudes of the correlation coefficients are larger during the ENSO developing phase for the two southern regions but during the ENSO decaying phase for the two western regions. The fraction of ozone variance that is linked to the Niño 3.4 index is as high as 36% (i.e., $r \sim 0.6$ in

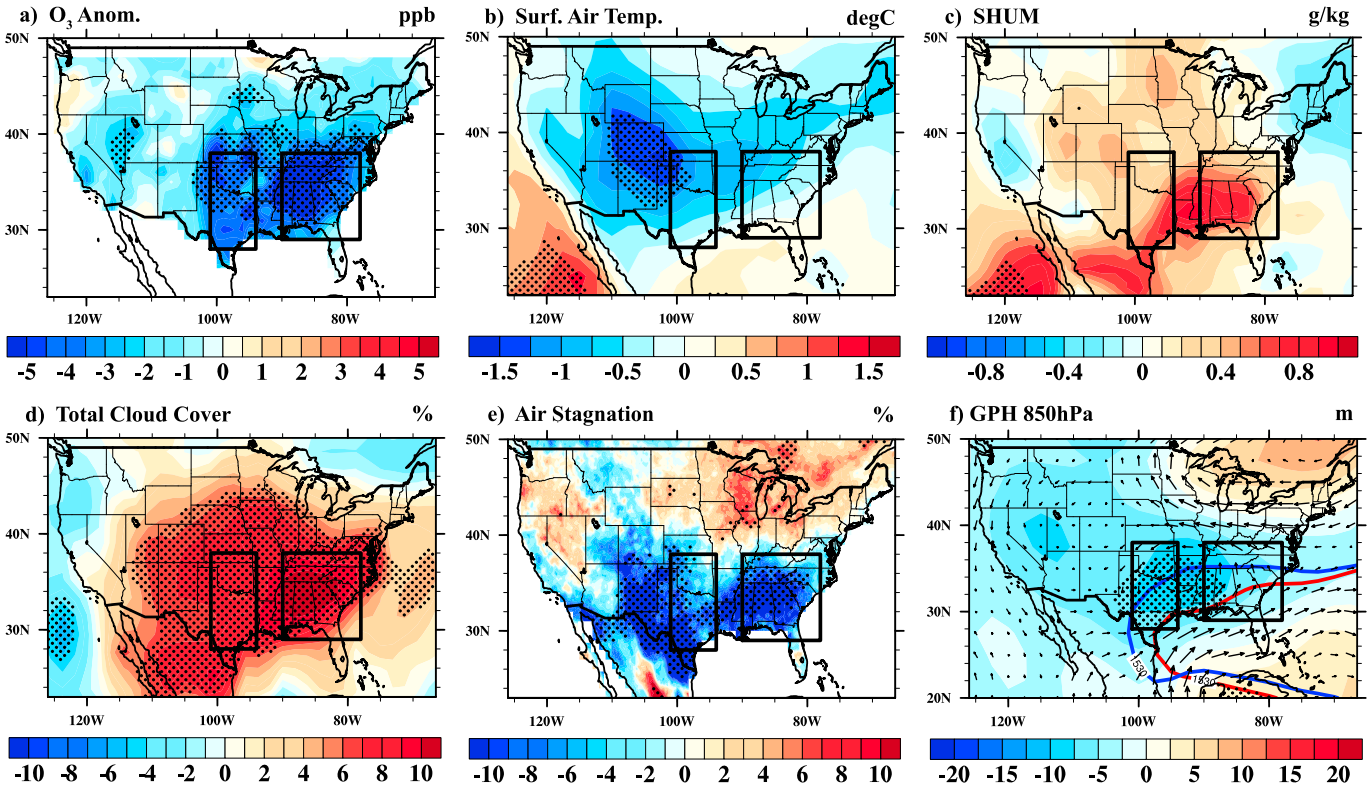

Figure 3. The difference in the composite of (a) surface ozone anomalies (ppb), (b) surface air temperature anomalies (degrees Celsius), (c) 2 m specific humidity anomalies (g/kg), (d) total cloud cover anomalies (%), (e) air stagnation index anomalies (%), and (f) 850 hPa geopotential height anomalies (m) between El Niño and La Niña conditions for fall (SON_{-1}) during the developing ENSO phase. Figure 3f is composited with 850 hPa geopotential height (m) in El Niño (red solid line) and La Niña (blue solid line) conditions along with the difference in 850 hPa wind vector anomalies between El Niño and La Niña. Statistically significant deviations of 95% are stippled. Two regions (i.e., SE and SC) are marked as black rectangular boxes.

Figure 2b) for the SE region during the developing phase of ENSO. This lagged analysis is consistent with the straight seasonal correlations (Figure 2a) in that the relationship with ENSO is strongest during fall of the developing ENSO phase for the two southern regions and during the winter to spring of the decaying ENSO phase for the two western regions.

In order to test the field significance of the correlations over the selected four regions, we conducted a Monte Carlo test following *Livezey and Chen* [1983]. The method is described in detail in the supporting information. The test shows that the correlation is significant in the two western regions during the winter to spring of the decaying ENSO phase and in the two southern regions during fall of the developing ENSO phase (see Table S1 in the supporting information). The correlation is significant in the south central U.S. (i.e., SC) during the spring of the decaying ENSO phase (i.e., MAM_0) and in the southeastern U.S. (i.e., SE) during the spring of the developing ENSO phase (i.e., MAM_{-1}), but their absolute values are smaller than those during fall of the developing ENSO phase (i.e., SON_{-1}) (see Figure 2b). Therefore, we focus our discussion on two southern regions during fall of the developing ENSO phase (i.e., SON_{-1}).

To gain some understanding of possible mechanisms whereby ENSO influences U.S. surface ozone, we collect monthly mean meteorological variables that are generally associated with extreme ozone pollution. We then generated a composite graph for these quantities and surface ozone showing the El Niño minus La Niña conditions. Using the oceanic Niño index (http://ggweather.com/enso/oni.htm) and the criteria set by National Atmospheric and Oceanic Administration (NOAA), we identified six El Niño episodes (1994–1995, 1997–1998, 2002–2003, 2004–2005, 2006–2007, and 2009–2010) and seven La Niña episodes (1995–1996, 1998–1999, 1999–2000, 2000–2001, 2007–2008, 2010–2011, and 2011–2012) during the analysis period 1993–2013. Note that we choose composite plots here because they can explicitly allow us to identify the changes in ozone anomalies as well as relevant meteorological variables associated with two ENSO

phases (i.e., the developing and decaying phase) in the most straightforward manner. The differences during fall of the ENSO developing phases are shown in Figure 3. A large reduction of ozone concentrations (1 to 10 ppb) occurs in the two southern regions (marked) during El Niño years compared to La Niña years (Figure 3a). Lower surface air temperatures (Figure 3b) might cause this through reduced kinetics rates and/or isoprene emissions, but reductions in the SE region are small, −1°C at most. Higher water vapor (Figure 3c) may increase ozone loss through HO_x reactions, but in these high-VOC environments the HO_x budget is not simply related to water vapor. Large increases in cloudiness (Figure 3d), +10% in SE, will clearly reduce photochemical production of ozone. The decrease in stagnation index (Figure 3e) is extensive over both SC and SE regions and will reduce surface ozone buildup.

It is difficult to assess which meteorological changes (Figures 3b–3e), if any, might be causing the ozone changes. Similarity in geographic patterns of ozone change may be accidental because much of the ozone variability is driven by the location in pollution sources and not just the meteorology [see, e.g., *Schnell et al*., 2014, Figure 4]. Nevertheless, cloud cover and stagnation index differences are uniformly broad across both SC and SE regions. Both temperature decreases and humidity increases would drive ozone decreases in the eastern U.S. [*Camalier et al*., 2007; *Huang et al*., 2007]. Another meteorological factor, the 850 hPa geopotential height (Figure 3f), shows the well-known ENSO displacement of the Bermuda high-pressure system, which brings more Gulf of Mexico air into the SE and SC regions. This shift can explain in part the increase in humidity and cloud cover but also lower levels of ozone typically found in the subtropical marine boundary layer.

For the two western regions, the ENSO impact on surface ozone concentration is largest and negative during the winter to spring of the ENSO decaying phases. We examine the differences in meteorological conditions between the El Niño composite and the La Niña composite in this season in Figure 4, in parallel with Figure 3 except the change in seasons and replacement of the 850-hPa geopotential with 200 hPa zonal wind ($m\,s^{-1}$) and 925 hPa meridional wind ($m\,s^{-1}$). In the SW region, the lower surface ozone appears to be related to cooler temperatures (Figure 4b), higher specific humidity (Figure 4c), and higher cloudiness (Figure 4d), but these changes are small in the sections of SW with largest ozone decreases. The increase in air stagnation days (Figure 4e) is small but would tend opposite, increasing ozone. The large-scale meteorological shifts indicate a stronger subtropical jet stream (Figure 4f) and stronger surface southerly winds (Figure 4g) from the tropical Pacific up the West Coast. The springtime jet is often linked with rapid transport of East Asian pollutant to the western U.S., contrary to the observed ozone decrease. The increased southerly flow up the coast will bring ozone-poor air from the Eastern Pacific and may be a cause of the decrease. In addition, the decrease in wild fires during El Niño events [*Swetnam and Betancourt*, 1990] may contribute to decreases in the concentrations of ozone precursors (e.g., anthropogenic NO_x and VOC), likely leading to decreases in ozone over this region.

The NW region is relatively unpolluted [see *Schnell et al*., 2014, Figure 4], and the springtime reduction in surface ozone during the El Niño (Figure 4a) is likely due to greater photochemical losses associated with higher temperatures (Figure 4b) and specific humidity (Figure 4c). Cloud cover changes (Figure 4d) are small, and increased stagnation (Figure 4e) would even tend to reduce ozone in unpolluted regions where chemistry near the surface tends to destroy ozone. The increased southerly flow along the coast does not extend to NW. Previous modeling studies [*Zeng and Pyle*, 2005; *Lin et al*., 2015; *Strode et al*., 2015] find that the stratosphere-troposphere exchange of ozone is enhanced over the western U.S. during the spring following La Niña years (i.e., 1999, 2008, and 2011) and that these higher ozone concentrations can reach the surface. These increases, consistent with the negative shifts in Figure 4a, occur primarily over the mountainous regions, a much larger area than the NW and SW regions. Moreover, they are broadly consistent with the observed negative shift from 117°W to 100°W seen in Figure 4a. Similar changes in ozone and all examined meteorological variables are also found in the winter (DJF_0) of the decaying ENSO phase over this region (Figure S1).

High levels of surface ozone concentration can threaten human health. Therefore, it is also important to know the probability that the ENSO can increase or decrease the occurrence of those extreme events. For this purpose, we compare in Figure 5 the probability density function (PDF) of anomalous MDA8 surface ozone mixing ratio between El Niño and La Niña conditions. The PDFs were constructed for the four studied regions using the daily MDA8 ozone anomalies on 1° × 1° grid cells from the months with the top 10% (i.e., El Niño

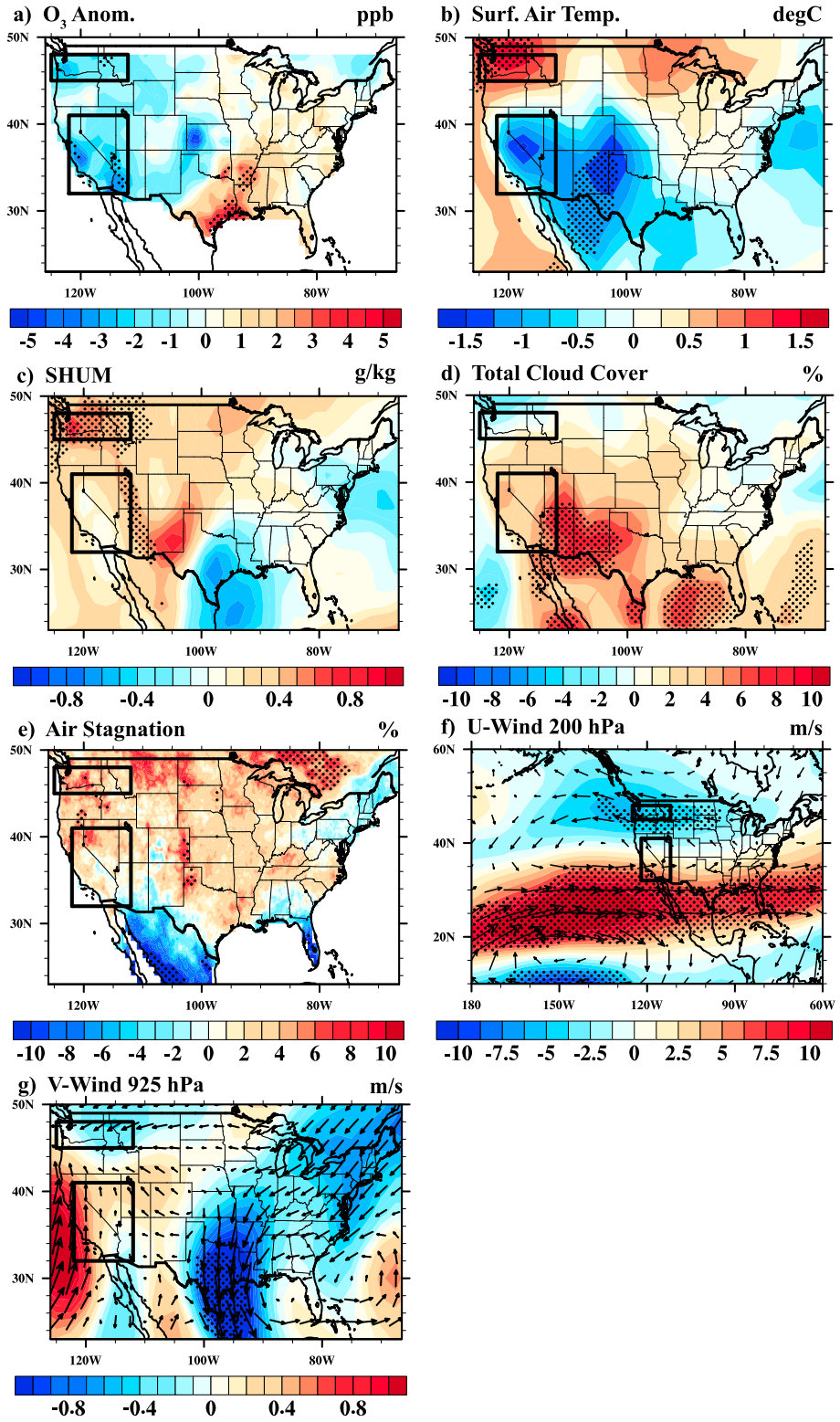

Figure 4. The difference in the composite of (a) surface ozone anomalies (ppb), (b) surface air temperature (degrees Celsius), (c) 2 m specific humidity (g/kg), (d) total cloud cover (%), (e) air stagnation index (%), (f) 200 hPa zonal wind ($m\ s^{-1}$), and (g) 925 hPa meridional wind ($m\ s^{-1}$) between El Niño and La Niña conditions for the spring (MAM_0) during the decaying ENSO phase. Figures 4f and 4g are composited with the difference in wind vector anomalies at respective pressure levels between El Niño and La Niña. Statistically significant deviations of 95% are stippled. Two regions (i.e., SW and NW) are marked as black rectangular boxes.

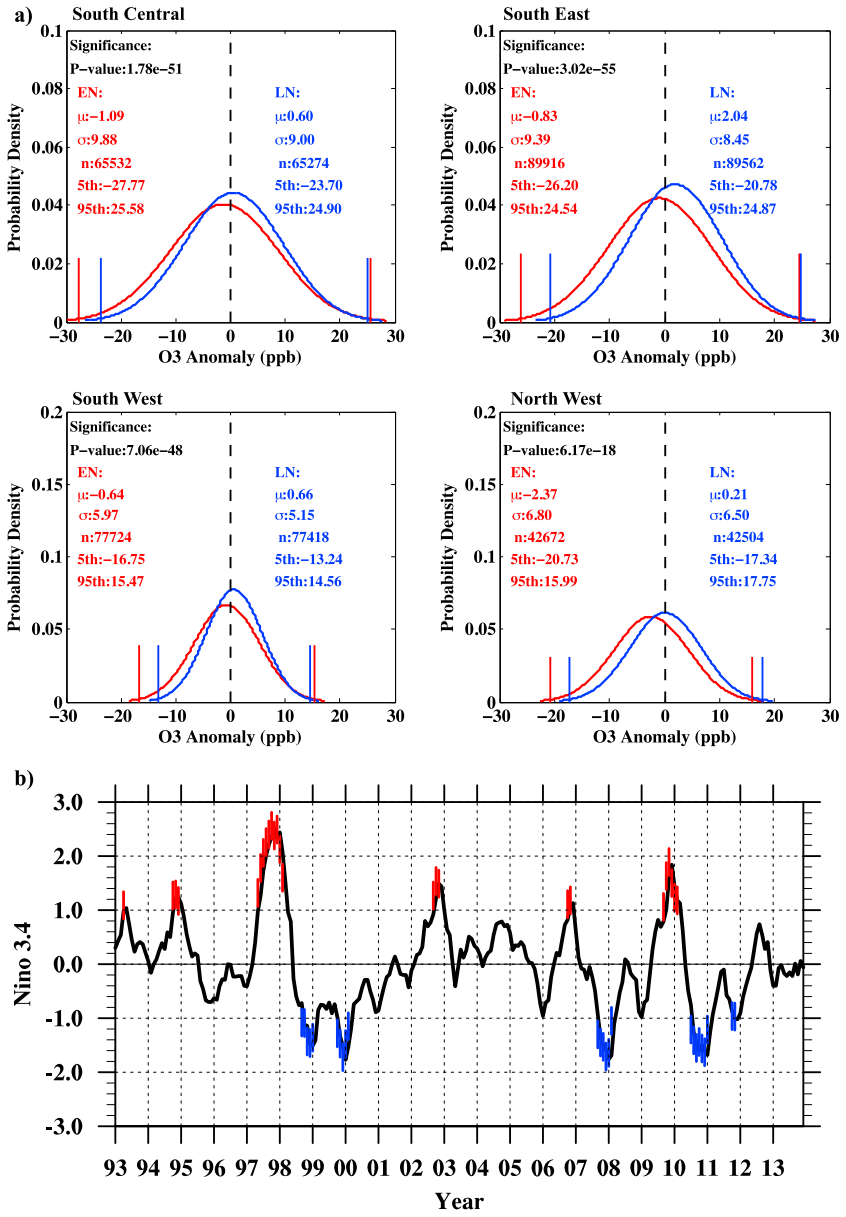

Figure 5. (a) The probability density function (PDF) of daily MDA8 ozone anomalies (ppb) on 1° × 1° grid cells from the months with the top 10% (i.e., El Niño conditions marked as red in Figure 5b) and bottom 10% (i.e., La Niña conditions marked as blue in Figure 5b) values of (b) the monthly Niño 3.4 index during 1993–2013 for four U.S. regions (i.e., South Central, South East, South West, and North West). The mean (μ), standard deviation (σ), sample size (n), and the 5th and 95th percentiles of PDFs for El Niño (red) and La Niña (blue) conditions are labeled in each panel. The p value from the two-sample Kolmogorov-Smirnov test is provided at the 95% significance level. The 5th and 95th percentiles of PDFs are marked as short vertical lines.

conditions marked as red in Figure 5b) and bottom 10% (i.e., La Niña conditions marked as blue in Figure 5b) values of the monthly Niño 3.4 index during 1993–2013. We conducted the two-sample Kolmogorov-Smirnov test at the 95% significance level. The small p values present in Figure 5 suggest that the PDF of daily ozone anomalies between El Niño and La Niña condition is statistically significantly different from each other at the 95% significance level, generally related with a significant shift in the location parameter (mean) of the PDFs. In other words, the mean of the PDF tends to shift toward the above-average side during the La Niña condition but toward the below-average side during the El Niño condition. This tendency can be observed in all four regions (Figure 5a). The 5th percentile of daily ozone anomalies increases about 2–5 ppb for all

four regions from the El Niño to La Niña condition, suggesting that there is higher chance of the occurrence of clean days during the El Niño condition than during the La Niña condition. On the other hand, ENSO contributes to influence on the 95th percentile of daily surface ozone. For example, the daily ozone mixing ratio increases approximately 1.76 ppb for the NW region when transiting from the El Niño to the La Niña condition. This tendency indicates that the occurrence of extreme high ozone events during the La Niña condition is higher than during the El Niño condition for the NW region. The increase of extreme high ozone episodes in the NW regions is likely due to the greater stratosphere-troposphere exchange of ozone during La Niña conditions than during El Niño conditions. The increase of extreme ozone episodes is not obvious for the other three regions because of small difference in changes of 95th percentile of daily ozone abundance over these regions. The PDF during the El Niño is wider than that during the La Niña for all four regions, indicated by a higher variance of ozone anomalies during the El Niño.

4. Conclusions

This study examines the influence of ENSO on the year-to-year variations of U.S. surface ozone concentrations during 1993–2013. In general, U.S. surface ozone concentrations decrease during El Niño episodes but increase during La Niña episodes. The study concludes that the amplitude of surface ozone changes through the ENSO cycle varies from 0.4 ppb (continent-wide average) to 1.8 ppb in the southeastern U.S. on a monthly basis, which is significant and important and should be considered when defining baseline surface ozone levels for the purposes of air quality regulation. The ENSO influence is largest over two southern and two western regions of the U.S. Interestingly, the strongest ENSO influence on ozone concentrations occurs neither during the season of the highest ozone concentration (i.e., boreal summer; JJA) nor during the season of the peak ENSO intensity (i.e., boreal winter; DJF) except for the northwestern U.S. Through a lead-lagged analysis and a Monte Carlo test, we found that the ENSO influences are strongest during fall of the ENSO developing phase for the two southern U.S. regions (i.e., the SE and SW) with the amplitude of surface ozone changes of 1.4–1.7 ppb and during the winter to spring of the ENSO decaying phase for the two western regions with surface ozone changes of 1.0–1.4 ppb.

This different seasonality implies that the ENSO-driven mechanisms that affect the surface ozone concentrations are different between the southern and western U.S. We are able to show that in the southern U.S., where meteorological conditions are favorable for ozone production and loss, ENSO affects mean ozone by altering its chemical processes during warm seasons (i.e., summer and fall). In the western U.S., where the Pacific jet streams enter and are known to be strongly affected by ENSO during the cold seasons (i.e., winter and spring), ENSO affects mean ozone by altering its transport [*Ropelewski and Halpert*, 1987; *Halpert and Ropelewski*, 1992]. In addition, ENSO contributes to influence on the number of extreme ozone episodes, particularly in the NW region, due in part to the enhanced stratosphere-troposphere exchange of ozone during La Niña conditions. We recognize that the meteorology induced mechanism on ozone changes explored in this work is not necessarily a complete attribution because the ENSO-driven changes in ozone and meteorological variables are averaged over a large time period. Nevertheless, the spatial dependence and the seasonality of ENSO impacts on U.S. ozone variability we identify can not only advance our understanding of the sources of the U.S. surface ozone variations but also improve our ability to better prepare for the occurrence of extreme ozone events.

Acknowledgments
The authors thank two anonymous reviewers and Editor Joel Thornton for their constructive comments that have helped improve the paper. This research was supported by the National Science Foundation's Climate and Large Scale Dynamics Program under grants AGS-1505145 and AGS-1233542. The NCEP/NCAR Reanalysis data set is downloaded from www.esrl.noaa.gov/psd/, the Niño 3.4 index from http://www.esrl.noaa.gov/psd/gcos_wgsp/Timeseries/Nino34, and the air stagnation index from https://www.ncdc.noaa.gov/societal-impacts/air-stagnation/overview. The ozone data are archived at University of California, Irvine, and can be accessed via ftp after requesting them from the corresponding author.

References

An, S.-I., and B. Wang (2000), Interdecadal change of the structure of the ENSO mode and its impact on the ENSO frequency, *J. Clim.*, *13*, 2044–2055.

Bjerknes, J. (1969), Atmospheric teleconnections from the equatorial Pacific, *Mon. Weather Rev.*, *18*, 820–829.

Bloomer, B. J., J. W. Stehr, C. A. Piety, R. J. Salawitch, and R. R. Dickerson (2009), Observed relationships of ozone air pollution with temperature and emissions, *Geophys. Res. Lett.*, *36*, L09803, doi:10.1029/2009GL037308.

Camalier, L., W. Cox, and P. Dolwick (2007), The effects of meteorology on ozone in urban areas and their use in assessing ozone trends, *Atmos. Environ.*, *41*(33), 7127–7137, doi:10.1016/j.atmosenv.2007.04.061.

Chandra, S., J. R. Ziemke, W. Min, and W. G. Read (1998), Effects of 1997–1998 El Niño on tropospheric ozone and water vapor, *Geophys. Res. Lett.*, *25*, 3867–3870, doi:10.1029/98GL02695.

Chandra, S., J. R. Ziemke, P. K. Bhartia, and R. V. Martin (2002), Tropical tropospheric ozone: Implications for dynamics and biomass burning, *J. Geophys. Res.*, *107*(D14), 4188, doi:10.1029/2001JD000447.

Chandra, S., J. R. Ziemke, B. N. Duncan, T. L. Diehl, N. J. Livesey, and L. Froidevaux (2009), Effects of the 2006 El Niño on tropospheric ozone and carbon monoxide: Implications for dynamics and biomass burning, *Atmos. Chem. Phys.*, *9*, 4239–4249.

Cooper, O. R., R. S. Gao, D. Tarasick, T. Leblanc, and C. Sweeney (2012), Long-term ozone trends at rural ozone monitoring sites across the United States, 1990–2010, *J. Geophys. Res.*, *117*, D22307, doi:10.1029/2012JD018261.

Doherty, R. M., D. S. Stevenson, C. E. Johnson, W. J. Collins, and M. G. Sanderson (2006), Tropospheric ozone and El Niño–Southern Oscillation: Influence of atmospheric dynamics, biomass burning emissions, and future climate change, *J. Geophys. Res.*, *111*, D19304, doi:10.1029/2005JD006849.

Enfield, D. B. (1989), El Niño, past and present, *Rev. Geophys.*, *27*(1), 159–187, doi:10.1029/RG027i001p00159.

Halpert, M. S., and C. F. Ropelewski (1992), Surface temperature patterns associated with the Southern Oscillation, *J. Clim.*, *5*, 577–593.

Huang, H.-C., X.-Z. Liang, K. E. Kunkel, M. Caughey, and A. Williams (2007), Seasonal simulation of tropospheric ozone over the Midwestern and northeastern United States: An application of a coupled regional climate and air quality modelling system, *J. Appl. Met. Clim.*, *46*, 945–960, doi:10.1175/JAM2521.1.

Jaffe, D., H. Price, D. Parrish, A. Goldstein, and J. Harris (2003), Increasing background ozone during spring on the west coast of North America, *Geophys. Res. Lett.*, *30*(12), 1613, doi:10.1029/2003GL017024.

Kalnay, V. E., et al. (1996), The NCEP/NCAR 40-year reanalysis project, *Bull. Am. Meteorol. Soc.*, *77*, 437–471.

Kao, H.-Y., and J.-Y. Yu (2009), Contrasting eastern-Pacific and central-Pacific types of ENSO, *J. Clim.*, *22*, 615–632, doi:10.1175/2008JCLI2309.1.

Leibensperger, E. M., L. J. Mickley, and D. J. Jacob (2008), Sensitivity of US air quality to mid-latitude cyclone frequency and implications of 1980–2006 climate change, *Atmos. Chem. Phys.*, *8*, 7075–7086.

Liang, Y.-C., J.-Y. Yu, M.-H. Lo, and C. Wang (2015), The changing influence of El Niño on the Great Plains low-level jet, *Atmosph. Sci. Lett.*, *16*, 512–517, doi:10.1002/asl.590.

Liang, Y.-C., C.-C. Chou, J.-Y. Yu, and M.-H. Lo (2016), Mapping the locations of asymmetric and symmetric discharge responses in global rivers to the two types of El Niño, *Environ. Res. Lett.*, *11*, 4, doi:10.1088/1748-9326/11/4/044012.

Lin, M., L. W. Horowitz, S. J. Oltmans, A. M. Fiore, and S. Fan (2014), Tropospheric ozone trends at Mauna Loa Observatory tied to decadal climate variability, *Nat. Geosci.*, *7*, 136–143, doi:10.1038/NGEO2066.

Lin, M., A. M. Fiore, L. W. Horowitz, A. O. Langford, S. J. Oltmans, D. Tarasick, and H. E. Reider (2015), Climate variability modulates western US ozone air quality in spring via deep stratospheric intrusions, *Nat. Commun.*, *6*, 7105, doi:10.1038/ncomms8105.

Livezey, R. E., and W. Y. Chen (1983), Statistical field significance and its determination by Monte Carlo techniques, *Mon. Weather Rev.*, *111*, 46–59.

Mo, K. C. (2010), Interdecadal modulation of the impact of ENSO on precipitation and temperature over the United States, *J. Clim.*, *23*, 3639–3656.

Olsen, M. A., K. Wargan, and S. Pawson (2016), Tropospheric column ozone response to ENSO in GEOS-5 assimilation of OMI and MLS ozone data, *Atmos. Chem. Phys.*, *16*, 7091–7103, doi:10.5194/acp-16-7091-2016.

Randel, W. J., and J. B. Cobb (1994), Coherent variations of monthly mean total ozone and lower stratospheric temperature, *J. Geophys. Res.*, *99*, 5433–5477, doi:10.1029/93JD03454.

Randel, W. J., and A. M. Thompson (2011), Interannual variability and trends in tropical ozone derived from SAGE II satellite data and SHADOZ ozonesondes, *J. Geophys. Res.*, *116*, D07303, doi:10.1029/2010JD015195.

Rasmussen, E. M., and T. H. Carpenter (1982), Variations in tropical sea surface temperature and surface wind fields associated with the Southern Oscillation/El Niño, *Mon. Weather Rev.*, *110*, 354–384.

Ropelewski, C. F., and M. S. Halpert (1987), North American precipitation and temperature patterns associated with the El Niño/Southern Oscillation (ENSO), *Mon. Weather Rev.*, *114*, 2352–2362.

Schnell, J. L., C. D. Holmes, A. Jangam, and M. J. Prather (2014), Skill in forecasting extreme ozone pollution episodes with a global atmospheric chemistry model, *Atmos. Chem. Phys.*, *14*, 7721–7739, doi:10.5194/acp-14-7721-2014.

Schnell, J. L., et al. (2015), Use of North American and European air quality networks to evaluate global chemistry–climate modeling of surface ozone, *Atmos. Chem. Phys.*, *15*, 10,581–10,596, doi:10.5194/acp-15-10581-2015.

Shen, L., L. J. Mickley, and A. P. K. Tai (2015), Influence of synoptic patterns on surface ozone variability over the eastern United States from 1980 to 2012, *Atmos. Chem. Phys.*, *15*, 10,925–10,938, doi:10.5194/acp-15-10925-2015.

Strode, S. A., J. M. Rodriguez, J. A. Logan, O. R. Cooper, J. C. Witte, L. N. Lamsal, M. Damon, B. Van Aartsen, S. D. Steenrod, and S. E. Strahan (2015), Trends and variability in surface ozone over the United States, *J. Geophys. Res. Atmos.*, *120*, 9020–9042, doi:10.1002/2014JD022784.

Sudo, K., and M. Takahashi (2001), Simulation of tropospheric ozone changes during 1997–1998 El Niño: Meteorological impact on tropospheric photochemistry, *Geophys. Res. Lett.*, *28*, 4091–4094, doi:10.1029/2001GL013335.

Swetnam, T. W., and J. L. Betancourt (1990), Fire-Southern Oscillation relations in the southwestern United States, *Science*, *249*, 1017–1021.

Wang, J. X. L., and J. K. Angell (1999), Air Stagnation Climatology for the United States (1948–1998), NOAA/Air Resources Laboratory ATLAS, No.1.

Yu, J.-Y., and Y. Zou (2013), The enhanced drying effect of Central-Pacific El Niño on US winter, *Environ. Res. Lett.*, *8*, 1, doi:10.1088/1748-9326/8/1/014019.

Yu, J.-Y., Y. Zou, S. T. Kim, and T. Lee (2012), The changing impact of El Niño on US winter temperatures, *Geophys. Res. Lett.*, *39*, L15702, doi:10.1029/2012GL052483.

Zeng, G., and J. A. Pyle (2005), Influence of El Niño Southern Oscillation on stratosphere/troposphere exchange and the global tropospheric ozone budget, *Geophys. Res. Lett.*, *32*, L01814, doi:10.1029/2004GL021353.

Ziemke, J. R., and S. Chandra (2003), La Niña and El Niño-induced variabilities of ozone in the tropical lower atmosphere during 1970–2001, *Geophys. Res. Lett.*, *30*(3), 1142, doi:10.1029/2002GL016387.